Coupled-channel effects in hadronic transitions in heavy-quarkonium systems

Hong-Yi Zhou
Department of Physics, Tsinghua University, Beijing 100084, China

Yu-Ping Kuang
Newman Laboratory of Nuclear Studies, Cornell University, Ithaca, New York 14853;
Chinese Center of Advanced Science and Technology (World Laboratory), P. O. Box 8730, Beijing 100080, China;
*Department of Physics, Tsinghua University, Beijing 100084, China;**
and Institute of Theoretical Physics, Academia Sinica, Beijing 100080, China
(Received 10 September 1990)

A systematic calculation of the coupled-channel effects in hadronic transitions in the $c\bar{c}$ and $b\bar{b}$ systems is given. The unitarized quark model based on the $^3P_0$ quark-pair-creation mechanism is adopted as the coupled-channel model. The emitted pions can now be produced both from the conventional Okubo-Zweig-Iizuka- (OZI) forbidden process described by QCD multipole-gluon emissions and from the light-quark loop through an OZI-allowed process described by the quark-pair-creation model. There is interference between the two kinds of transition amplitudes. Taking the experimental values of $\Gamma(\psi'\to J/\psi\pi\pi)$ and $d\Gamma(\psi'\to J/\psi\pi\pi)/dM_{\pi\pi}$ as inputs to determine the two unknown parameters in the theory, we predict the transition rates and $M_{\pi\pi}$ distributions in the $b\bar{b}$ system. The obtained rates for $\Upsilon'\to\Upsilon\pi\pi$, $\Upsilon''\to\Upsilon\pi\pi$, $\Upsilon''\to\Upsilon'\pi\pi$ and the distribution $d\Gamma(\Upsilon'\to\Upsilon\pi\pi)/dM_{\pi\pi}$ are in good agreement with the experiments. For $d\Gamma(\Upsilon''\to\Upsilon\pi\pi)/dM_{\pi\pi}$, the present theory does give a bigger low-$M_{\pi\pi}$ distribution than the pure QCD multipole expansion does, but it is still too small to fit the CLEO data.

I. INTRODUCTION

Because of the requirement of unitarity, coupled-channnel effects should, in principle, be considered in the theory of heavy quarkonia. At present it is still not possible to study coupled-channel effects from the first principles of QCD. Phenomenological studies of coupled-channel corrections to the energy spectra, leptonic widths, electromagnetic transition rates, etc., in the ψ and Υ families have been made in different models and the results are successful [1,2]. For hadronic transitions in the $c\bar{c}$ and $b\bar{b}$ systems, a systematic study of the coupled-channel contributions does not exist yet. The existing systematic calculations are based on QCD multipole expansion and the naive single-channel model [3–5]. This kind of calculation gives successful predictions for the hadronic transition rates in the $c\bar{c}$ and $b\bar{b}$ systems and the $\pi\pi$ invariant-mass ($M_{\pi\pi}$) distributions in $\psi'\to J/\psi+\pi+\pi$ and $\Upsilon'\to\Upsilon+\pi+\pi$ [3–8]. However, recent CLEO experiments [9] on the $\pi\pi$ invariant-mass distribution in $\Upsilon''\to\Upsilon+\pi^+\pi^-$ give a severe challenge to the conventional theory. The CLEO data show a double-peaked shape of $d\Gamma(\Upsilon''\to\Upsilon\pi^+\pi^-)/dM_{\pi\pi}$, while the QCD multipole expansion gives only one peak at the high-$M_{\pi\pi}$ region. There are several attempts to explain the CLEO data by assuming different dominant transition mechanisms in $\Upsilon''\to\Upsilon+\pi+\pi$. Voloshin [10] and Truong [11] assumed the existence of a four-quark state Υ_1 having nearly the same mass as Υ'' and coupling strongly to $\Upsilon''\pi$ and $\Upsilon\pi$, and the dominant transition mechanism is suggested to be $\Upsilon''\to\Upsilon_1+\pi\to\Upsilon+\pi+\pi$ which enhances the low-$M_{\pi\pi}$ distribution. Bélanger, DeGrand, and Moxhay [12] combined this mechanism with the final-state $\pi\pi$ interactions and got a double-peaked shape of $d\Gamma(\Upsilon''\to\Upsilon\pi\pi)/dM_{\pi\pi}$ but the low-$M_{\pi\pi}$ peak is not at the desired position. This assumption can be directly tested by searching for Υ_1 in the decay $\Upsilon(4S)\to\Upsilon_1+\pi$, whose branching ratio is roughly of the order of 1% [10,11]. So far no positive result has been reported. A different suggestion by Lipkin and Tuan [13] is that the transition is dominated by $\Upsilon''\to B+\bar{B}\to B^*+\bar{B}+\pi\to B+\bar{B}+\pi+\pi\to\Upsilon+\pi+\pi$, so that the transition amplitude is proportional to $\mathbf{k}_1\cdot\mathbf{k}_2$ ($\mathbf{k}_1$ and $\mathbf{k}_2$ are three-momenta of the two pions) and this leads to an $M_{\pi\pi}$ distribution symmetric in low- and high-$M_{\pi\pi}$ values. Moxhay [14] further assumed that the above mechanism is dominated by a constant amplitude rather than being proportional to $\mathbf{k}_1\cdot\mathbf{k}_2$ and it is large enough (comparable to the multipole amplitude) to have a significant interference with the multipole amplitude. He was able to make the $M_{\pi\pi}$ distribution fit the CLEO data by adjusting the magnitude of the constant amplitude. The Lipkin-Tuan and Moxhay amplitudes are actually parts of the total coupled-channel contributions. They should be studied together with other coupled-channel contributions and should be examined in $\psi'\to J/\psi+\pi+\pi$ and $\Upsilon'\to\Upsilon+\pi+\pi$ as well. This study should also be consistent with the coupled-channel study of other heavy-quarkonium processes such as energy spectra, leptonic widths, etc. Once a realistic coupled-channel model is taken, these amplitudes are completely calculable. Therefore a systematic calculation of the coupled-channel effects in hadronic transitions is of special interest for making clear whether or not the Lipkin-Tuan or Moxhay mechanism can really be realized. Furthermore, hadronic transitions from states above the threshold can also be

measured in recent experiments [15]. A theoretical study of $\psi(3770)\to J/\psi+\pi+\pi$ considering state mixings (a part of coupled-channel effects) has been given in Ref. [4]. A thorough investigation of this kind of process also needs a systematic calculation of coupled-channel effects.

In this paper we shall take a well-accepted realistic coupled-channel model and give a systematic calculation of coupled-channel effects in hadronic transitions. We shall first give a general formalism and then calculate specifically the $\pi\pi$ transitions from a spin-triplet S state to a lower-lying spin-triplet S state in the $c\bar{c}$ and $b\bar{b}$ systems. Other hadronic transition processes can be considered in the same way from our general formalism. In the coupled-channel formalism the emitted pions can still be produced from the conventional Okubo-Zweig-Iizuka-(OZI) forbidden process described by the QCD multipole-gluon emissions but with coupled-channel corrections. In addition, once light-quark loops are introduced, the emitted pions can also be produced from the light-quark loop through an OZI-allowed process. This contains the amplitudes considered by Lipkin-Tuan [13] and Moxhay [14]. One of the well-accepted successful models, the unitarized quark model [2] (UQM) based on the $^3P_0$ quark-pair-creation (QPC) mechanism [16], will be adopted as the coupled-channel model in this paper. We take this model for the following reasons: (a) the parameters in this model are carefully adjusted so that the model gives a better fit to the $c\bar{c}$ and $b\bar{b}$ spectra, leptonic widths, etc., and (b) the QPC model has been shown to give not bad results even for OZI-allowed production of light mesons [16,17], which we have to be concerned with in our calculation of the second-kind pion-emissions process. The above-mentioned amplitudes of the second-kind pion emissions depend solely on the model of QPC, so that there are no free parameters in these amplitudes when the model is given. When we use the soft-pion approach to the hadronization matrix element in the multipole amplitudes (the first kind of pion emissions), as we did in Ref. [3], there are two unknown parameters, namely, the magnitude and phase of the unknown constant c_1 [3], which affect the final results. We shall take the well-measured experimental values of $\Gamma(\psi'\to J/\psi\pi\pi)$ and $d\Gamma(\psi'\to J/\psi\pi\pi)/dM_{\pi\pi}$ as inputs to determine the two parameters and make predictions for the transition rates and $M_{\pi\pi}$ distributions in the $b\bar{b}$ system. We shall see that the obtained rates of $\Upsilon'\to\Upsilon+\pi+\pi$, $\Upsilon''\to\Upsilon+\pi+\pi$, $\Upsilon''\to\Upsilon'+\pi+\pi$ and the distribution $d\Gamma(\Upsilon'\to\Upsilon\pi\pi)/dM_{\pi\pi}$ all fit the new experiments [6,8] better than the previous naive results in Ref. [3]. The distribution $d\Gamma(\Upsilon''\to\Upsilon\pi\pi)/dM_{\pi\pi}$ also gets improved from the coupled-channel corrections. The low-$M_{\pi\pi}$ distribution increases a little, but it is still too small to fit the CLEO data. This small improvement comes mostly from the state mixings in the multipole amplitudes, while the corresponding amplitudes considered by Lipkin-Tuan and Moxhay are actually smaller than the multipole ones by an order of magnitude in the present model. The smallness of the second-kind pion-emission amplitudes is caused by the nodes of the Υ'' wave function since the Υ''-B-$\bar{B}$ coupling is determined by the overlapping integral between the three wave functions. Therefore the conjecture made by Lipkin-Tuan and Moxhay that these amplitudes are large is not realized in the present model. Our result does not support their suggestions. At present the explanation of the CLEO data is still not clear. It seems that the physics is more complicated than any of the suggested singly dominant mechanisms.

This paper is organized as follows. In Sec. II we give a general formalism of hadronic transition amplitudes including coupled-channel effects. Section III contains the details of the calculations and results of the S-state-to-S-state $\pi\pi$ transition rates and $M_{\pi\pi}$ distributions in the $c\bar{c}$ and $b\bar{b}$ systems. Some discussions of the results and a concluding remark are given in Sec. IV.

II. HADRONIC TRANSITIONS IN COUPLED-CHANNEL THEORY

For giving a general formulation of hadronic transitions in the coupled-channel theory, we first briefly review the main points of the UQM. Let Φ be the heavy-quarkonium composed of a heavy quark Q and its antiquark $\bar{Q}$ (e.g., J/ψ, ψ', Υ, Υ', etc.) and $\mathcal{D}$ be the heavy-flavored meson composed of Q ($\bar{Q}$) and a light quark $\bar{q}$ (q) [e.g., D ($\bar{D}$), D^* ($\bar{D}^*$), B ($\bar{B}$), B^* ($\bar{B}^*$), etc.]. In the UQM [2] the whole Hilbert space is divided into two sectors: namely, the confined sector $|\Phi_0;\lambda\rangle$ labeled by the discrete quantum number λ and the continuous sector $|\mathcal{D}\bar{\mathcal{D}};\nu\rangle$ labeled by the continuous quantum number (say the momentum) ν. The state $|\Phi_0;\lambda\rangle$ is just the eigenstate of the Hamiltonian H_0 in the naive single-channel theory with eigenvalue M_λ^0 (the bare mass); i.e.,

$$H_0|\Phi_0;\lambda\rangle=M_\lambda^0|\Phi_0;\lambda\rangle\ , \tag{1}$$

and the state $|\mathcal{D}\bar{\mathcal{D}};\nu\rangle$ is a state with two freely moving mesons $\mathcal{D}$ and $\bar{\mathcal{D}}$, which is the eigenstate of the kinetic-energy Hamiltonian H_0^c with energy eigenvalue E_ν; i.e.,

$$H_0^c|\mathcal{D}\bar{\mathcal{D}};\nu\rangle=E_\nu|\mathcal{D}\bar{\mathcal{D}};\nu\rangle\ . \tag{2}$$

The total Hamiltonian H of the system contains H_0, H_0^c, and the quark-pair-creation Hamiltonian $H_{\rm QPC}$ which determines the OZI-allowed Φ-$\mathcal{D}$-$\bar{\mathcal{D}}$ vertex and mixes the two sectors. H can be written as

$$H=\begin{bmatrix}H_0 & 0\\ 0 & H_0^c\end{bmatrix}+\begin{bmatrix}0 & H_{\rm QPC}^\dagger\\ H_{\rm QPC} & 0\end{bmatrix}\begin{matrix}\}\text{confined channels}\\ \}\text{continuous channels}\ .\end{matrix} \tag{3}$$

Note that

$$\langle\Phi_0;\lambda|H_{\rm QPC}|\Phi_0;\lambda'\rangle=0$$

and

$$\langle\mathcal{D}\bar{\mathcal{D}};\nu|H_{\rm QPC}|\mathcal{D}\bar{\mathcal{D}};\nu'\rangle=0\ .$$

With $H_{\rm QPC}$ introduced, there will be the virtual process $\Phi\to\mathcal{D}+\bar{\mathcal{D}}\to\Phi'$ which causes the state mixing and energy shift (self-energy Π coming from the virtual $\mathcal{D}$ loop) of the quarkonium Φ. The physical quarkonium state $|\Phi;\lambda\rangle$ is the eigenstate of the total Hamiltonian H with

energy eigenvalue M_λ; i.e.,

$$H|\Phi;\lambda\rangle = M_\lambda|\Phi;\lambda\rangle \ . \tag{4}$$

$|\Phi;\lambda\rangle$ can be written as a superposition of the states $|\Phi_0;\lambda\rangle$ and $|\mathcal{D}\bar{\mathcal{D}};\nu\rangle$:

$$|\Phi;\lambda\rangle = \sum_{\lambda'} a_{\lambda\lambda'}|\Phi_0;\lambda'\rangle + \int d\nu\, c_\lambda(\nu)|\mathcal{D}\bar{\mathcal{D}};\nu\rangle \ . \tag{5}$$

It is understood that the second term in (5) contains the contributions of $\mathcal{D}$ ($\bar{\mathcal{D}}$) composed of Q ($\bar{Q}$) and all possible $\bar{q}$ (q). From (1)–(5) we can easily see that

$$\sum_{\lambda'} [(M_\lambda - M_\lambda^0)\delta_{\lambda\lambda'} - \Pi_{\lambda\lambda'}(M_\lambda)]a_{\lambda\lambda'} = 0 \ , \tag{6}$$

where $\Pi_{\lambda\lambda'}$ is the self-energy contributed by the $\mathcal{D}$ loops, and for quarkonium states below the threshold [2]:

$$\Pi_{\lambda\lambda'} = -\int \frac{\langle\Phi_0;\lambda|H_{\rm QPC}^\dagger|\mathcal{D}\bar{\mathcal{D}};\nu\rangle\langle\mathcal{D}\bar{\mathcal{D}};\nu|H_{\rm QPC}|\Phi_0;\lambda'\rangle}{M_\lambda - E_\nu} d\nu \ . \tag{7}$$

Equation (6) means that M_λ is obtained by diagonalizing the mass matrix:

$$M_{\lambda\lambda'} = M_\lambda^0\delta_{\lambda\lambda'} + \Pi_{\lambda\lambda'} \ . \tag{8}$$

Let $\alpha_{\lambda\lambda'}$ be the matrix diagonalizing $M_{\lambda\lambda'}$. The mixing coefficient $a_{\lambda\lambda'}$ is related to $\alpha_{\lambda\lambda'}$ by

$$a_{\lambda\lambda'} = N_\lambda \alpha_{\lambda\lambda'}^T \ , \tag{9}$$

where [2]

$$N_\lambda = \left[1 + \int \frac{\langle\mathcal{D}\bar{\mathcal{D}};\nu|H_{\rm QPC}|\Phi_0;\lambda\rangle}{M_\lambda - E_\nu}\right|^2 d\nu\Bigg]^{(-1/2)} \tag{10}$$

is a normalization coefficient and N_λ^2 determines the probability of finding the confined sector $|\Phi_0;\lambda\rangle$ in the physical state $|\Phi;\lambda\rangle$. The values of α's and N_λ's for various $c\bar{c}$ and $b\bar{b}$ states are given in Ref. [2]. The mixing coefficient $c_\lambda(\nu)$ is related to $a_{\lambda\lambda'}$ by [2]

$$c_\lambda(\nu) = \sum_{\lambda'} a_{\lambda\lambda'}\langle\mathcal{D}\bar{\mathcal{D}};\nu|H_{\rm QPC}|\Phi_0\lambda'\rangle/(M_\lambda - E_\nu) \ . \tag{11}$$

The above consideration is sufficient for studying the spectra, leptonic widths, etc., of heavy quarkonia when the model for $\langle\mathcal{D}\bar{\mathcal{D}};\nu|H_{\rm QPC}|\Phi_0;\lambda\rangle$ is given [2]. However, as far as hadronic transitions are concerned, we should consider further various mechanisms of pion emissions. Apart from the well-known OZI-forbidden multipole-gluon-emission mechanism, the pion can also be produced from the light-quark line in $\mathcal{D}$ or $\bar{\mathcal{D}}$ through an OZI-allowed mechanism. In principle the OZI-allowed pion emission is also mediated by gluons, but at present there is no proper method of calculating the OZI-allowed soft-pion emissions from the first principles of QCD. Now the OZI-allowed Φ-$\mathcal{D}$-$\bar{\mathcal{D}}$ vertex is phenomenologically represented by $\langle\mathcal{D}\bar{\mathcal{D}};\nu|H_{\rm QPC}|\Phi_0;\lambda\rangle$ with success [2] and the same treatment has been applied to light-meson systems in Refs. [16] and [17]. The calculation in Ref. [17] shows that with a universal potential model and coupling strength for calculating the matrix elements of $H_{\rm QPC}$, the model works pretty well for the mesons ϕ and K, and even the results for π and ρ are not so bad (the deviation of the results from experiments is less than a factor of 2). The reason for the success of the constituent quark potential model in studying light mesons has been discussed by Gromes [18]. Thus, in this paper, we take the same QPC model to treat the OZI-allowed pion-emission vertex. As we shall see in Sec. III, this kind of transition amplitude is smaller than the multipole one by an order of magnitude. Therefore a factor-of-2 uncertainty in the calculation of OZI-allowed pion emission does not affect the total amplitude much, and thus our final results are reliable. The OZI-allowed pion emission appears in the form

$$\langle\mathcal{D}\bar{\mathcal{D}}\pi;\nu'|H_{\rm QPC}|\mathcal{D}\bar{\mathcal{D}};\nu\rangle \ , \tag{12}$$

in which the pion is produced by $H_{\rm QPC}$ from the light-quark line in $\mathcal{D}$ or $\bar{\mathcal{D}}$ and the other $\bar{\mathcal{D}}$ or $\mathcal{D}$ serves as a spectator.

In Ref. [19] a general formula for the S-matrix element in the framework of QCD multipole expansion is given, in which the OZI-forbidden soft-gluon-emission vertex is described by the Hamiltonian

$$H_2 = -\mathbf{d}_a\cdot\mathbf{E}^a(\mathbf{X},t) - \mathbf{m}_a\cdot\mathbf{B}^a(\mathbf{X},t) + \cdots \ , \tag{13}$$

where $\mathbf{d}_a$ and $\mathbf{m}_a$ are the color electric and magnetic dipole moments of Φ, $\mathbf{E}^a$ and $\mathbf{B}^a$ are the color electric and magnetic fields, and $\mathbf{X}$ is the coordinate of the center of mass of Φ. Now we have an additional OZI-allowed pion-emission mechanism described by $H_{\rm QPC}$. Let

$$H_{\rm pair} \equiv H_{\rm QPC} + H_{\rm QPC}^\dagger \ . \tag{14}$$

Our general formula for the S-matrix element [19] can now be generalized to

$$\langle f|S|i\rangle = -i2\pi\delta(M_f + \omega_f - M_i)$$

$$\times\left\langle f\left|(H_2+H_{\rm pair})\frac{1}{M_i - \hat{H}_0 + i\partial_0 - H_1}(H_2+H_{\rm pair})\cdots\frac{1}{M_i - \hat{H}_0 + i\partial_0 - H_1}(H_2+H_{\rm pair})\right|i\right\rangle \ , \tag{15}$$

where M_i and M_f are, respectively, the physical masses of the initial- and final-state quarkonia, ω_f is the energy of the final-state pions,

$$\hat{H}_0 = \begin{cases} H_0 & \text{confined channels} , \\ H_0^c & \text{continuous channels} , \end{cases}$$

$$H_1 = Q_a A_0^a(\mathbf{X},t) ,$$

with Q_a the color charge and A_0^a the gluon gauge potential ($H_1=0$ in color-singlet states), and $i\partial_0$ is understood to operate only on the gluon fields. As has been mentioned, although both the OZI-forbidden and -allowed pion-emission processes are mediated by gluons in QCD, we take here different approaches to the different mechanisms through H_2 and H_{pair}. Each of H_2 and H_{pair} describe one kind of pion emission, so that there is no double counting in (15). Note that in (15) the H_{pair} contribute to both the $\Phi-\mathcal{D}-\bar{\mathcal{D}}$ vertices and the pion-emission vertices such as (12).

For isospin-conserving $\pi\pi$ transitions the multipole part is dominated by $E1$-$E1$ gluon emissions; i.e., H_2 is dominated by the first term in (13) and only two H_2's are to be taken into account in (15) [20]. In this case the two pions can be produced either by the two H_2's or by two H_{QPC}'s but not both, since the two gluons in the two H_2's can only convert into two pions (not one pion) due to isospin conservation. Therefore the two pion-emission mechanisms are separated. Later on we shall use the short terms ME amplitude and QPC amplitude for the OZI-forbidden pion-emission (multipole expansion) and the OZI-allowed pion-emission (quark-pair-creation) transition amplitudes, respectively. In (15), apart from the two H_2's in the ME amplitudes and the two H_{QPC}'s in the QPC amplitudes, there can be extra H_{pair}'s with equal number of $H_{\text{QPC}}^\dagger$'s and H_{QPC}'s. We know that a pair of adjacent $H_{\text{QPC}}^\dagger H_{\text{QPC}}$ just creates a meson loop which belongs to the self-energy correction. In the following calculations we shall identify the physical masses of Φ and $\mathcal{D}$ with the experimentally measured masses, so that all self-energy contributions are understood to be already included and thus those adjacent $H_{\text{QPC}}^\dagger H_{\text{QPC}}$ pairs should be ignored. The quarkonium states $|i\rangle$ and $|f\rangle$ are physical states including both the confined and the continuous sectors [cf. (5)]. For the QPC amplitudes only the continuous sector contributes. It is easy to see from (11) that

$$\int d\nu\, c_\lambda(\nu)|\mathcal{D}\bar{\mathcal{D}};\nu\rangle = (M_\lambda - \hat{H}_0)^{-1} H_{\text{QPC}} \sum_{\lambda'} a_{\lambda\lambda'}|\Phi_0;\lambda'\rangle . \tag{16}$$

Therefore, for $\pi\pi$ transition from $|\Phi;\lambda_i\rangle$ to $|\Phi;\lambda_f\rangle$, (15) can be written as

$$\begin{aligned}
&\langle \Phi\pi\pi;\lambda_f \mathbf{k}_1\mathbf{k}_2|S|\Phi;\lambda_i\rangle \\
&\quad = -i2\pi\delta(M_f+\omega_1+\omega_2-M_i) \\
&\qquad \times \sum_{\lambda_i'\lambda_f'} a_{\lambda_i\lambda_i'} a_{\lambda_f\lambda_f'} \left\langle \Phi_0\pi\pi;\lambda_f'\mathbf{k}_1\mathbf{k}_2 \right| \Bigg[H_2 \frac{1}{M_i-\hat{H}_0+i\partial_0-H_1} H_2 \\
&\qquad\quad + H_{\text{QPC}}^\dagger \frac{1}{M_i-\hat{H}_0+i\partial_0-H_1} H_2 \frac{1}{M_i-\hat{H}_0+i\partial_0-H_1} H_2 \frac{1}{M_i-\hat{H}_0} H_{\text{QPC}} \\
&\qquad\quad + H_2 \frac{1}{M_i-\hat{H}_0+i\partial_0-H_1} H_{\text{QPC}}^\dagger \frac{1}{M_i-\hat{H}_0+i\partial_0-H_1} H_2 \frac{1}{M_i-\hat{H}_0} H_{\text{QPC}} \\
&\qquad\quad + H_{\text{QPC}}^\dagger \frac{1}{M_i-\hat{H}_0+i\partial_0-H_1} H_2 \frac{1}{M_i-\hat{H}_0+i\partial_0-H_1} H_{\text{QPC}} \frac{1}{M_i-\hat{H}_0+i\partial_0-H_1} H_2 \\
&\qquad\quad + H_{\text{QPC}}^\dagger \frac{1}{M_i-\hat{H}_0} H_{\text{QPC}} \frac{1}{M_i-\hat{H}_0} H_{\text{QPC}} \frac{1}{M_i-\hat{H}_0} H_{\text{QPC}} \Bigg] \Big| \Phi_0;\lambda_i' \Big\rangle ,
\end{aligned} \tag{17}$$

where ω_1 and ω_2 are the energies of the two final-state pions, respectively. The first term in (17) is just the conventional ME amplitude taking into account the state mixings. Its diagram is shown in Fig. 1(a). This amplitude has been calculated in Ref. [21] and the obtained rates in the $b\bar{b}$ system are larger than the experiments. We shall see that the inclusion of coupled-channel contributions [other terms in (17)] makes the final results in good agreement with experiments. The second term in (17) represents multipole-gluon emissions from the continuous sector and the diagrams are shown in Figs. 1(b) and 1(c). The third and fourth terms are amplitudes with one gluon emitted from the continuous sector and the other gluon emitted from the confined sector as depicted in Fig. 1(d). The last term in (17) gives the QPC amplitudes, and their diagrams are shown in Figs. 1(e) and 1(f). The diagrams in Fig. 1(e) correspond to the processes considered by Lipkin and Tuan [13] and Moxhay [14]. If we take into account only the S-state $\mathcal{D}$ ($\bar{\mathcal{D}}$) meson contributions in Fig. 1(e) [e.g., $\bar{B}(B)$, $\bar{B}^*$ (B^*)], the emitted pions should be in the P wave due to parity conservation and the amplitude is proportional to $\mathbf{k}_1\cdot\mathbf{k}_2$, which is just

the Lipkin-Tuan amplitude. If the $\mathcal{D}_2$ ($\bar{\mathcal{D}}_2$) meson between the two pions in Fig. 1(e) is taken to be the P-wave excitation $\bar{B}^{**}$ ($\bar{B}^{**}$), the emitted pion can be in the S wave and the amplitude is independent of $\mathbf{k}_1$ and $\mathbf{k}_2$, which is just the constant amplitude considered by Moxhay. Therefore both the Lipkin-Tuan and Moxhay mechanisms belong to Fig. 1(e), and there are many other coupled-channel amplitudes that should be calculated

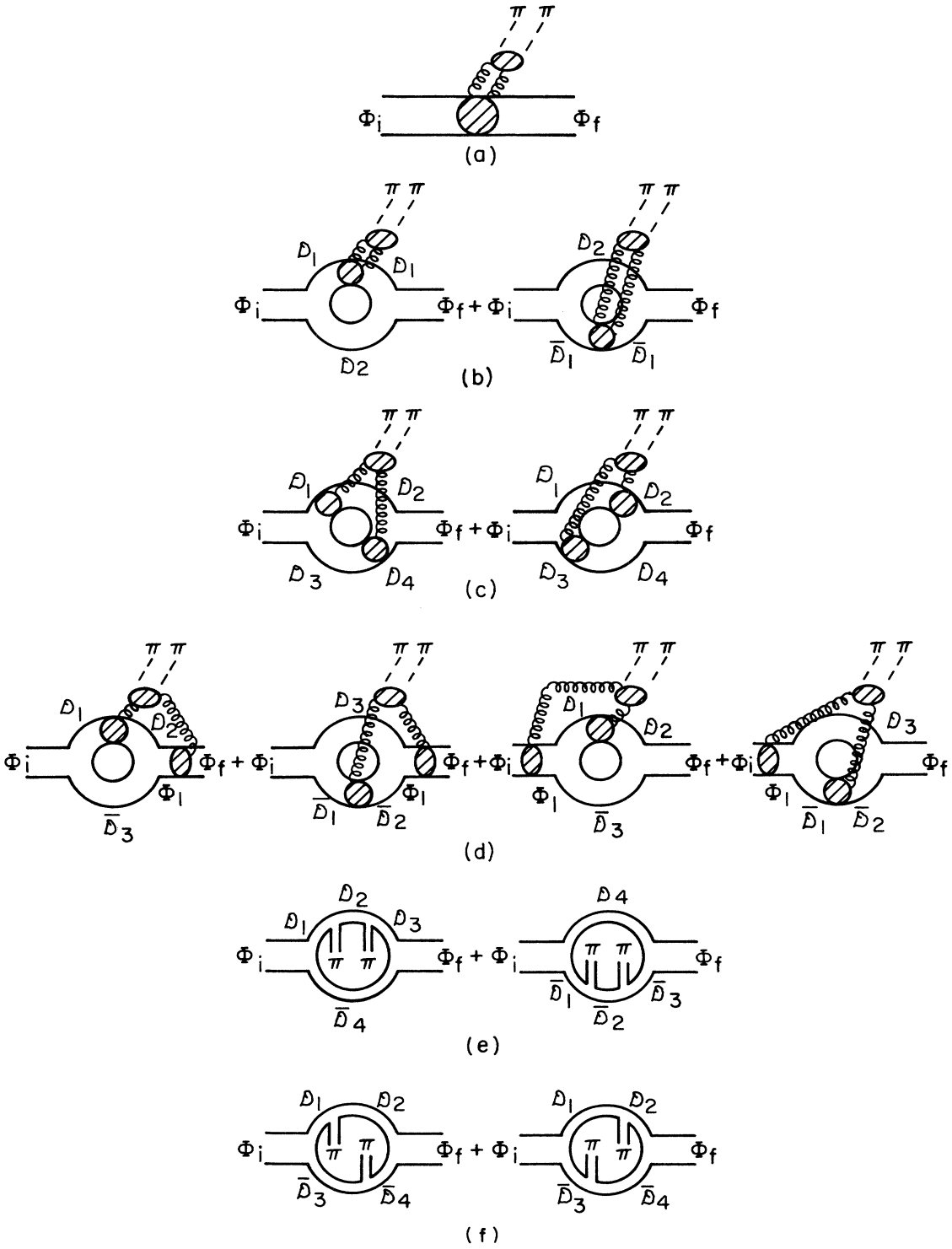

FIG. 1. Feynman diagrams for various terms in Eq. (17). The solid lines, spiral lines, and dashed lines stand for quarks, gluons, and pions, respectively.

simultaneously.

In the UQM [2], the model for $H_{\rm QPC}$ is taken to be the $^3P_0$ quark-pair-creation model formulated in Ref. [16]. We need to consider here the creation of light-quark pairs $q\bar{q}$ (q can be u, d, or s) with which a meson A goes to two mesons B and C. The operator $H_{\rm QPC}$ is expressed as [17]

$$H_{\rm QPC}=\gamma_{\rm QPC}\sum_{l_z,s_z}\sum_{\alpha,\beta}\sum_{i,j}\int d^3\mathbf{p}_1 d^3\mathbf{p}_2\,\delta^3(\mathbf{p}_1+\mathbf{p}_2)\langle 1l_z,1s_z|00\rangle \times\mathbf{Y}_1^{l_z}(\mathbf{p}_1-\mathbf{p}_2)\Phi^{s_z}_{\alpha i\beta j} \times a^\dagger_{\alpha i}(\mathbf{p}_1)b^\dagger_{\beta j}(\mathbf{p}_2)\ , \tag{18}$$

where $\gamma_{\rm QPC}$ is a constant denoting the strength of QPC, $a^\dagger$ ($b^\dagger$) is the creation operator of the light quark q ($\bar{q}$) labeled by the spin index α (β) and the SU(3)-flavor index i (j), $\Phi^{s_z}_{\alpha i\beta j}$ represents the spin and flavor structure of the $q\bar{q}$ pair:

$$\Phi^{s_z}=\frac{1}{\sqrt{3}}(u\bar{u}+d\bar{d}+s\bar{s})\chi_1^{s_z}\ . \tag{19}$$

The state vector of the meson $A(B,C)$ can be written as

$$|A(B,C);\mathbf{k}\rangle=\int d^3\mathbf{q}\,\tilde{\psi}_{A(B,C)}(\mathbf{q})\Phi^{s_z}_{\alpha i\beta j}a'^\dagger_{\alpha i} \times(\mathbf{q}+\tfrac{1}{2}h_2\mathbf{k})b'^\dagger_{\beta j}(-\mathbf{q}+\tfrac{1}{2}h_1\mathbf{k})|0\rangle\ . \tag{20}$$

Here $a'^\dagger(b'^\dagger)$ can be the creation operator of a heavy or light quark (antiquark), $\tilde{\psi}_{A(B,C)}(\mathbf{q})$ is the momentum representation of the meson wave function $\psi_{A(B,C)}(\mathbf{x})$, $\mathbf{k}$ is the momentum of the meson $A(B,C)$, and

$$h_1\equiv\frac{2m_2}{m_1+m_2},\quad h_2\equiv\frac{2m_1}{m_1+m_2}\ , \tag{21}$$

with m_1 and m_2 the masses of the quark and antiquark, respectively. The matrix element $\langle BC|H_{\rm QPC}|A\rangle$ can then be calculated from (18) and (20). Apart from some kinematical spin and flavor factors given explicitly in Ref. [2], the dynamical factor of $\langle BC|H_{\rm QPC}|A\rangle$ is determined by an overlapping integral:

$$I_m(ABC)=\int d^3\mathbf{q}\,\mathbf{Y}_1^m(2\mathbf{q}+h_1\mathbf{k})\tilde{\psi}_A \times(\mathbf{q}-\tfrac{1}{2}h_2\mathbf{k})\tilde{\psi}^*_B(\mathbf{q})\tilde{\psi}^*_C(\mathbf{q})\ , \tag{22}$$

where $\mathbf{k}$ is the decay momentum. The wave functions $\tilde{\psi}_A,\tilde{\psi}_B,\tilde{\psi}_C$ should be calculated from a certain dynamical model. It has been argued in Ref. [2] that the final results are not very sensitive to the details of this model, and they take the following potential model [22] to calculate the wave functions in (22):

$$\begin{aligned}&V(r)=\frac{8\pi}{25}\frac{1}{r\ln(r/\mu)}+ar-be^{-r/c}\ ,\\ &\mu=(\Lambda e^{0.5772})^{-1},\quad \Lambda=0.5\ \text{GeV}\ ,\\ &a=0.787\ \text{GeV/fm},\quad b=1.378\ \text{GeV}\ ,\\ &c=1.20\ \text{GeV}^{-1}\ ,\\ &m_c=1.90\ \text{GeV},\quad m_b=5.25\ \text{GeV}\ ,\\ &m_u=m_d=0.336\ \text{GeV},\quad m_3=0.620\ \text{GeV}\ .\end{aligned} \tag{23}$$

The coupling constants $\gamma_{\rm QPC}=3.03$ is determined from the best fit of the data [2]. This $\gamma_{\rm QPC}$ is almost universal for heavy and light mesons. With the model and parameters fixed, the self-energy $\Pi_{\lambda\lambda'}$ can be calculated, and after identifying the physical mass M_λ with the measured mass, the bare mass spectra M^0_λ can be determined. In the UQM the potential for the heavy-$Q\bar{Q}$ systems is chosen to fit the bare mass spectra and in Ref. [2] it is chosen to be the Lichtenberg-Wills potential [23] but with different parameters [2]:

$$\begin{aligned}&V(r)=\frac{8\pi}{25}\frac{(1-\lambda r)^2}{r\ln(\lambda r)}+A\ ,\\ &\lambda=\Lambda e^{0.5772},\quad \Lambda=350\ \text{MeV},\quad A=-850\ \text{MeV}\ ,\\ &m_c=1.90\ \text{GeV},\quad m_b=5.21\ \text{GeV}\ .\end{aligned} \tag{24}$$

In our calculation, we mainly follow these models, while in the calculation of the Φ-$\mathcal{D}$-$\bar{\mathcal{D}}$ vertices in Figs. 1(b)–1(f) a corrected Φ wave function considering (24) is used.

Our general formula (15) can be applied to other hadronic transition processes and even some other decay processes [19,24] with similar considerations.

III. CALCULATION OF TRANSITIONS IN THE $c\bar{c}$ AND $b\bar{b}$ SYSTEMS

The matrix elements in (17) can be evaluated by inserting intermediate states. For the ME amplitudes, after the first gluon emission, the intermediate state contains a soft gluon and a quark-antiquark pair in the color octet. It is difficult to treat this strongly interacting three-body system from the first principles of QCD. As what we have done in Ref. [3], we take the string vibrational states [25] to imitate these intermediate states. According to Ref. [25], the potential for the string vibrational states differs from the one for the normal $Q\bar{Q}$ states only by a known modification of the piece linear in r. Now the intermediate states should be taken to be the physical states, since we have ignored the adjacent $H^\dagger_{\rm QPC}H_{\rm QPC}$ pairs in (17). We know that for the normal $Q\bar{Q}$ states the potential (24) fits the bare mass spectra while the physical spectra (measured masses) can be well fitted by the potential (23). Therefore we shall take the potential (23) with its linear piece modified according to Ref. [25] to calculate the

spectra of the physical string vibrational states. We shall identify the lowest vibrational states with the small structure at 4.03 GeV by adjusting the strength of an extra Coulomb piece in the potential representing the screening effect [25].

The first term in (17) [Fig. 1(a)] has already been calculated in Ref. [21]. For spin-triplet S-state-to-S-state transitions it is

$$\mathcal{M}^{(a)}_{\rm ME}=\frac{g_E^2}{6}\sum_{n,l,n',l'}\sum_{K,L}a_{n_i0nl}a_{n_f0n'l'}\frac{\langle\Phi_{0;n'l'}|x_j|\Phi^v;KL\rangle\langle\Phi^v;KL|x_k|\Phi_0;nl\rangle}{M_i-E^v_{KL}}\langle\pi(\mathbf{k}_1)\pi(\mathbf{k}_2)|E^a_jE^a_k|0\rangle$$

$$=3\sum_{n,l,n',l'}\sum_{L,\bar{l},\bar{m}}a_{n_i0nl}a_{n_f0n'l'}(-1)^{L+m_f+1}(2L+1)[(2\bar{l}+1)(2l+1)(2l'+1)]^{1/2}\begin{bmatrix}\bar{l}&1&1\\ \bar{m}&m_i&-m_f\end{bmatrix}\begin{Bmatrix}1&1&\bar{l}\\ l&l'&1\end{Bmatrix}$$

$$\times\begin{Bmatrix}l&l'&\bar{l}\\ 1&1&L\end{Bmatrix}\begin{bmatrix}L&1&l\\ 0&0&0\end{bmatrix}\begin{bmatrix}L&1&l'\\ 0&0&0\end{bmatrix}[2(\omega_1)(2\omega_2)]^{-(1/2)}$$

$$\times[-\sqrt{3}c_1k_1^\mu k_{2\mu}\delta_{\bar{l}0}+2c_2(-1)^{\bar{m}}A^{\bar{l}}_{-\bar{m}}(\mathbf{k}_1,\mathbf{k}_2)\delta_{\bar{l}2}]f^L_{nln'l'}\ , \tag{25}$$

where n_i, n, n_f, n', and K are principal quantum numbers, l, l', and L are orbital-angular-momentum quantum numbers, m_i and m_f are magnetic quantum numbers of the total angular momenta in the initial and final state, $|\Phi^v;KL\rangle$ is the string vibrational state with energy eigenvalue E^v_{KL},

$$f^L_{nln'l'}\equiv\sum_K\frac{\int_0^\infty R_{n'l'}(r)R^v_{KL}(r)r^3\,dr\int_0^\infty R_{nl}(r)R^v_{KL}(r)r^3\,dr}{M_i-E^v_{KL}}\ , \tag{26}$$

with R and R^v the radial wave functions of Φ_0 and Φ^v, respectively, the rank $\bar{l}$ irreducible tensor $A^{\bar{l}}_{-\bar{m}}(\mathbf{k}_1,\mathbf{k}_2)$ is defined as

$$A^{\bar{l}}_{-\bar{m}}(\mathbf{k}_1,\mathbf{k}_2)=\sum_{m_1,m_2}(-1)^{\bar{m}}(2\bar{l}+1)^{1/2}\begin{bmatrix}1&1&\bar{l}\\ m_1&m_2&\bar{m}\end{bmatrix}\chi^{(1)}_{m_1}(\mathbf{k}_1)\chi^{(1)}_{m_2}(\mathbf{k}_2)\ , \tag{27}$$

with

$$\chi^{(1)}_0(\mathbf{k})=k_z,\quad \chi^{(1)}_{\pm1}(\mathbf{k})=\mp\frac{1}{\sqrt{2}}(k_x\pm ik_y)\ ,$$

and c_1,c_2 are two unknown constants in the soft-pion approach to the hadronization matrix element $\langle\pi(\mathbf{k}_1)\pi(\mathbf{k}_2)|E^a_iE^a_k|0\rangle$ [3]. In the free-gluon approximation [3]

$$|c_2|=3|c_1|\ , \tag{28}$$

(25) differs from the naive single-channel formula by the existence of the contributions from the transitions between various nl and $n'l'$ states. This causes a change of the $M_{\pi\pi}$ distribution. We know that for $n(n')\neq n_i(n_f)$, $l(l')\neq0$, the mixing coefficients $a_{n_i0nl}(a_{n_f0n'l'})$ are of second order of $\langle\mathcal{D}\bar{\mathcal{D}};\nu|H_{\rm QPC}|\Phi_0;\lambda\rangle$ and they are about an order of magnitude smaller than $a_{n_i0n_i0}(a_{n_f0n_f0})$ [2]. Therefore in (25) the main contributions are from various S-state-to-S-state, S-state-to-D-state, and D-state-to-S-state transitions, while the D-state-to-D-state transitions are negligibly small.

The second term in (17) represents two kinds of diagrams; namely, Figs. 1(b) and 1(c). Let us first consider Fig. 1(b). It contains two diagrams and their contributions are equal. Since each of the diagrams contains extra Φ-$\mathcal{D}$-$\bar{\mathcal{D}}$ vertices, the state-mixing contributions in this term are negligibly small compared with $\mathcal{M}^{(a)}_{\rm ME}$. Neglecting state mixings, the contribution of the two diagrams in Fig. 1(b) is

$$\mathcal{M}^{(b)}_{\rm ME}=-\frac{4}{3}\frac{\gamma^2_{\rm QPC}}{\pi^4}\sum_{\mathcal{D}_1,\bar{\mathcal{D}}_2,\mathcal{D}^v}\frac{1}{\sqrt{2\omega_1 2\omega_2}}(-1)^{m_f}(2S_{\mathcal{D}_1}+1)(2S_{\bar{\mathcal{D}}_2}+1)(2S_{\mathcal{D}_1\bar{\mathcal{D}}_2}+1)$$

$$\times\begin{bmatrix}0&1&1\\ 0&m_i&-m_f\end{bmatrix}\begin{Bmatrix}\frac{1}{2}&\frac{1}{2}&S_{\mathcal{D}_1}\\ \frac{1}{2}&\frac{1}{2}&S_{\bar{\mathcal{D}}_2}\\ 1&1&S_{\mathcal{D}_1\bar{\mathcal{D}}_2}\end{Bmatrix}^2\sqrt{3}c_1k_1^\mu k_{2\mu}\bar{f}^{(b)}_{n_i0n_f0}\ , \tag{29}$$

where $S_{\mathcal{D}}$, $S_{\bar{\mathcal{D}}}$, and $S_{\mathcal{D}\bar{\mathcal{D}}}$ are the spins of $\mathcal{D}$, $\bar{\mathcal{D}}$, and $\mathcal{D}\bar{\mathcal{D}}$ systems, respectively,

$$\bar{f}^{(b)}_{n_i 0 n_f 0} \equiv \int_0^\infty dk\, k^2 \frac{\left[\int_0^\infty R_{\mathcal{D}_1}(r) R^{v}_{\mathcal{D}}(r) r^3\, dr\right]^2 I_i(k) I_f(k)}{[M_i - E_{\mathcal{D}_1\bar{\mathcal{D}}_2}(k)][M_f - E_{\mathcal{D}_1\bar{\mathcal{D}}_2}(k)][M_i - E_{\mathcal{D}^v\bar{\mathcal{D}}_2}(k)]} , \tag{30}$$

in which $\mathcal{D}^v$ means the vibrational state,

$$E_{\mathcal{D}_1\bar{\mathcal{D}}_2} = (m^2_{\mathcal{D}_1} + k^2)^{1/2} + (m^2_{\bar{\mathcal{D}}_2} + k^2)^{1/2} , \tag{31}$$

$$I_{i(f)}(k) = \int_0^\infty dp\, p^2 \int_0^\infty dr\, r^2 R_{n_i 0(n_f 0)}(r) \tilde{R}_{\mathcal{D}_1}(p) \tilde{R}_{\bar{\mathcal{D}}_2}(p) \left[2p j_1(pr) j_1\left[\frac{h_q}{2} kr\right] + h_Q k j_0(pr) j_0\left[\frac{h_q}{2} kr\right]\right] , \tag{32}$$

with j_l the spherical Bessel function,

$$h_q = \frac{2m_Q}{m_Q + m_q}, \quad h_Q = \frac{2m_q}{m_Q + m_q} \tag{33}$$

and

$$\tilde{R}_{\mathcal{D}_1(\bar{\mathcal{D}}_2)}(p) = \int_0^\infty R_{\mathcal{D}_1(\bar{\mathcal{D}}_2)}(r) j_0(pr) r^2\, dr . \tag{34}$$

Here we have neglected the recoil of heavy mesons.

In Ref. [2] the contributions of the $l \neq 0$ excitations of $\mathcal{D}\bar{\mathcal{D}}$ [e.g., D^{**} ($\bar{D}^{**}$), $\bar{B}^{**}$ (B^{**})] are neglected in the calculations of the mass shifts, state mixings, etc., since it is argued that the contributions of such mesons to the Φ-$\mathcal{D}$-$\bar{\mathcal{D}}$ vertices are small [2]. To be consistent with Ref. [2], we also neglect the contribution of such mesons in our calculations of the Φ-$\mathcal{D}$-$\bar{\mathcal{D}}$ vertices. Now in Fig. 1(c) the mesons $\mathcal{D}_2, \bar{\mathcal{D}}_4$ at the vertex Φ_f-$\mathcal{D}_2$-$\bar{\mathcal{D}}_4$ must be the $l = 1$ excitations due to the selection rule $|\Delta l| = 1$ in the color electric-dipole gluon emission. Therefore, Fig. 1(c) should be ignored in our calculations. For the same reason, the third and fourth terms in (17) [Fig. 1(d)] should also be ignored. Hence the total ME amplitude is just

$$\mathcal{M}_{\rm ME} = \mathcal{M}^{(a)}_{\rm ME} + \mathcal{M}^{(b)}_{\rm ME} . \tag{35}$$

The last term in (17) [Figs. 1(e) and 1(f)] gives the QPC amplitudes. Similar to the case of $\mathcal{M}^{(b)}_{\rm ME}$, the state-mixing contributions in the QPC amplitudes are also negligibly small compared with $\mathcal{M}^{(a)}_{\rm ME}$ so that we neglect them. We also neglect the recoil of the heavy mesons, while the Lorentz boost factors $(m_\pi/\omega_1)^{1/2}$, $(m_\pi/\omega_2)^{1/2}$ will be taken into account for the pion wave functions.

Let us first consider the two diagrams in Fig. 1(e). Their contributions are equal. If we take into account only the contributions of the S-state $\mathcal{D}$ ($\bar{\mathcal{D}}$) mesons, the contribution of the two diagrams in Fig. 1(e) is

$$\begin{aligned}
\mathcal{M}^{(e)1}_{\rm QPC} = \frac{3\sqrt{3} m_\pi \gamma^4_{\rm QPC}}{\pi^9 \sqrt{\omega_1 \omega_2}} \sum_{\mathcal{D}_1\mathcal{D}_2,\mathcal{D}_3,\bar{\mathcal{D}}_4} (-1)^{m_f + S_{\mathcal{D}_2} + S_{\bar{\mathcal{D}}_4} + S_{\mathcal{D}_1\bar{\mathcal{D}}_4} + S_{\mathcal{D}_3\bar{\mathcal{D}}_4}} \\
\times (2S_{\mathcal{D}_1}+1)(2S_{\mathcal{D}_2}+1)(2S_{\mathcal{D}_3}+1)(2S_{\bar{\mathcal{D}}_4}+1)(2S_{\mathcal{D}_1\bar{\mathcal{D}}_4}+1)(2S_{\mathcal{D}_3\bar{\mathcal{D}}_4}+1) \\
\times \begin{Bmatrix} 0 & 1 & 1 \\ 0 & m_i & -m_f \end{Bmatrix} \begin{Bmatrix} S_{\mathcal{D}_1} & 1 & S_{\mathcal{D}_2} \\ \frac{1}{2} & \frac{1}{2} & \frac{1}{2} \end{Bmatrix} \begin{Bmatrix} S_{\mathcal{D}_2} & 1 & S_{\mathcal{D}_3} \\ \frac{1}{2} & \frac{1}{2} & \frac{1}{2} \end{Bmatrix} \begin{Bmatrix} 1 & 0 & 1 \\ 1 & S_{\mathcal{D}_1\bar{\mathcal{D}}_4} & 1 \end{Bmatrix} \\
\times \begin{Bmatrix} 1 & 0 & 1 \\ 1 & S_{\mathcal{D}_3\bar{\mathcal{D}}_4} & 1 \end{Bmatrix} \begin{Bmatrix} S_{\mathcal{D}_1} & S_{\mathcal{D}_3} & 0 \\ 1 & 1 & S_{\mathcal{D}_2} \end{Bmatrix} \begin{Bmatrix} 0 & S_{\mathcal{D}_1\bar{\mathcal{D}}_4} & S_{\mathcal{D}_3\mathcal{D}_4} \\ S_{\bar{\mathcal{D}}_4} & S_{\mathcal{D}_3} & S_{\mathcal{D}_1} \end{Bmatrix} \\
\times \begin{Bmatrix} 0 & 1 & 1 \\ 1 & S_{\mathcal{D}_3\bar{\mathcal{D}}_4} & S_{\mathcal{D}_1\bar{\mathcal{D}}_4} \end{Bmatrix} \begin{Bmatrix} \frac{1}{2} & \frac{1}{2} & S_{\mathcal{D}_1} \\ \frac{1}{2} & \frac{1}{2} & S_{\bar{\mathcal{D}}_4} \\ 1 & 1 & S_{\mathcal{D}_1\bar{\mathcal{D}}_4} \end{Bmatrix} \begin{Bmatrix} \frac{1}{2} & \frac{1}{2} & S_{\mathcal{D}_3} \\ \frac{1}{2} & \frac{1}{2} & S_{\bar{\mathcal{D}}_4} \\ 1 & 1 & S_{\mathcal{D}_3\bar{\mathcal{D}}_4} \end{Bmatrix} \bar{f}^{(e)1}_{n_i 0 n_f 0}(\omega_1) \mathbf{k}_1 \cdot \mathbf{k}_2 + (\mathbf{k}_1 \leftrightarrow \mathbf{k}_2) ,
\end{aligned} \tag{36}$$

where

$$\bar{f}^{(e)1}_{n_i 0 n_f 0}(\omega_1)\equiv\int_0^\infty dk\,k^2\frac{\int_0^\infty dp\,p^2\tilde{R}_{\mathcal{D}_1}(p)\tilde{R}_{\mathcal{D}_2}(p)\tilde{R}_\pi(p)\int_0^\infty dp\,p^2\tilde{R}_{\mathcal{D}_2}(p)\tilde{R}_{\mathcal{D}_3}(p)\tilde{R}_\pi(p)I_i(k)I_f(k)}{[M_i-E_{\mathcal{D}_1\bar{\mathcal{D}}_4}(k)][M_f-E_{\mathcal{D}_3\bar{\mathcal{D}}_4}(k)][M_i-\omega_1-E_{\mathcal{D}_2\bar{\mathcal{D}}_4}(k)]}\ , \tag{37}$$

and the definition of $\tilde{R}(p)$ is given in (34). In (36) we have neglected a small contribution from the rank-2 irreducible tensor $A^2_{-\bar{m}}(\mathbf{k}_1,\mathbf{k}_2)$. $\mathcal{M}^{(e)1}_{\rm QPC}$ is just the Lipkin-Tuan [13] amplitude, and its $\mathbf{k}_1\cdot\mathbf{k}_2$ dependence comes from the fact that the emitted pions are in the P wave due to parity conservation. If the meson $\mathcal{D}_2$ ($\bar{\mathcal{D}}_2$) in Fig. 1(e) is taken to be the $l=1$ excitation of $\mathcal{D}$ ($\bar{\mathcal{D}}$) [e.g., D^{**} ($\bar{D}^{**}$), $\bar{B}^{**}$ (B^{**})], the emitted pions can be in the S wave and the $\mathbf{k}_1\cdot\mathbf{k}_2$ dependence will no longer be there. We shall take into account this $l=1$ excitation contribution specially to the $\mathcal{D}_2$ ($\bar{\mathcal{D}}_2$) meson in Fig. 1(e) for the following reasons: (a) this is not inconsistent with Ref. [2], since the pion wave function is fatter than the wave function of Φ so that the $l=1$ excitation contribution in the π-$\mathcal{D}$-$\bar{\mathcal{D}}$ vertex is larger than that in the Φ-$\mathcal{D}$-$\bar{\mathcal{D}}$ vertex; (b) although in the π-$\mathcal{D}$-$\bar{\mathcal{D}}$ vertex the $l=1$ excitation contribution is smaller than the S state $\mathcal{D}$, $\bar{\mathcal{D}}$ contribution, the phase space of the former is larger than that of the latter due to the absence of $\mathbf{k}_1\cdot\mathbf{k}_2$, so that the final contributions of them are comparable; (c) it gives different $M_{\pi\pi}$ dependence of the rates. The result of the $l=1$ excitation to the two diagrams in Fig. 1(e) is

$$\begin{aligned}\mathcal{M}^{(e)2}_{\rm QPC}=&\frac{3\sqrt{3}m_\pi\gamma^4_{\rm QPC}}{\pi^9\sqrt{\omega_1\omega_2}}\sum_{\mathcal{D}_1,\mathcal{D}_2,\mathcal{D}_3,\bar{\mathcal{D}}_4}(-1)^{m_f+S_{\mathcal{D}_2}+S_{\bar{\mathcal{D}}_4}+S_{\mathcal{D}_1\bar{\mathcal{D}}_4}+S_{\mathcal{D}_3\bar{\mathcal{D}}_4}}\\
&\times(2S_{\mathcal{D}_1}+1)(2S_{\mathcal{D}_2}+1)(2S_{\mathcal{D}_3}+1)(2S_{\bar{\mathcal{D}}_4}+1)(2S_{\mathcal{D}_1\bar{\mathcal{D}}_4}+1)(2S_{\mathcal{D}_3\bar{\mathcal{D}}_4}+1)\\
&\times\begin{Bmatrix}0&1&1\\0&m_i&-m_f\end{Bmatrix}\begin{Bmatrix}S_{\mathcal{D}_1}&1&S_{\mathcal{D}_2}\\\frac{1}{2}&\frac{1}{2}&\frac{1}{2}\end{Bmatrix}\begin{Bmatrix}S_{\mathcal{D}_2}&1&S_{\mathcal{D}_3}\\\frac{1}{2}&\frac{1}{2}&\frac{1}{2}\end{Bmatrix}\begin{Bmatrix}1&0&1\\1&S_{\mathcal{D}_1\bar{\mathcal{D}}_4}&1\end{Bmatrix}\\
&\times\begin{Bmatrix}1&0&1\\1&S_{\mathcal{D}_3\bar{\mathcal{D}}_4}&1\end{Bmatrix}\begin{Bmatrix}S_{\mathcal{D}_1}&S_{\mathcal{D}_3}&0\\1&1&S_{\mathcal{D}_2}\end{Bmatrix}\begin{Bmatrix}0&S_{\mathcal{D}_1\bar{\mathcal{D}}_4}&S_{\mathcal{D}_3\bar{\mathcal{D}}_4}\\S_{\bar{\mathcal{D}}_4}&S_{\mathcal{D}_3}&S_{\mathcal{D}_1}\end{Bmatrix}\\
&\times\begin{Bmatrix}0&1&1\\1&S_{\mathcal{D}_3\bar{\mathcal{D}}_4}&S_{\mathcal{D}_1\bar{\mathcal{D}}_4}\end{Bmatrix}\begin{Bmatrix}\frac{1}{2}&\frac{1}{2}&S_{\mathcal{D}_1}\\\frac{1}{2}&\frac{1}{2}&S_{\bar{\mathcal{D}}_4}\\1&1&S_{\mathcal{D}_1\bar{\mathcal{D}}_4}\end{Bmatrix}\begin{Bmatrix}\frac{1}{2}&\frac{1}{2}&S_{\mathcal{D}_3}\\\frac{1}{2}&\frac{1}{2}&S_{\bar{\mathcal{D}}_4}\\1&1&S_{\mathcal{D}_3\bar{\mathcal{D}}_4}\end{Bmatrix}\bar{f}^{(e)2}_{n_i 0 n_f 0}(\omega_1)\mathbf{k}_1\cdot\mathbf{k}_2+(\mathbf{k}_1\leftrightarrow\mathbf{k}_2)\ ,\end{aligned} \tag{38}$$

where

$$\bar{f}^{(e)2}_{n_i 0 n_f 0}(\omega_1)$$

$$\equiv\int_0^\infty dk\,k^2\frac{4\int_0^\infty dp\,p^3\tilde{R}_{\mathcal{D}_1}(p)\tilde{R}_\pi(p)\int_0^\infty dx\,x^2R_{\mathcal{D}_2}(x)j_1(px)\int_0^\infty dp\,p^3\tilde{R}_{\mathcal{D}_3}(p)\tilde{R}_\pi(p)\int_0^\infty dx\,x^2R_{\mathcal{D}_2}(x)j_1(px)I_i(k)I_f(k)}{[M_i-E_{\mathcal{D}_1\bar{\mathcal{D}}_4}(k)][M_f-E_{\mathcal{D}_3\bar{\mathcal{D}}_4}(k)][M_i-\omega_1-E_{\mathcal{D}_2\bar{\mathcal{D}}_4}(k)]}\ , \tag{39}$$

with $\mathcal{D}_2$ being the $l=1$ excitation of $\mathcal{D}$. This is just the constant amplitude considered by Moxhay [14].

Note that there is no unknown parameter in $\mathcal{M}^{(e)1}_{\rm QPC}$ and $\mathcal{M}^{(e)2}_{\rm QPC}$ so that they are completely calculable.

The $l=1$ excitation contribution in Fig. 1(f) should be ignored since it appears in the Φ-$\mathcal{D}$-$\bar{\mathcal{D}}$ vertices. The result of the two diagrams in Fig. 1(f) is

$$\mathcal{M}^{(f)}_{\rm QPC}=\frac{3\sqrt{3}m_\pi\gamma^4_{\rm QPC}}{2\pi^9\sqrt{\omega_1\omega_2}}\sum_{\mathcal{D}_1,\mathcal{D}_2,\bar{\mathcal{D}}_3,\bar{\mathcal{D}}_4}(-1)^{m_f+S_{\mathcal{D}_2\bar{\mathcal{D}}_4}}[(-1)^{S_{\mathcal{D}_2}+S_{\bar{\mathcal{D}}_3}}+(-1)^{S_{\mathcal{D}_1}+S_{\bar{\mathcal{D}}_4}}]$$
$$\times(2S_{\mathcal{D}_1}+1)(2S_{\mathcal{D}_2}+1)(2S_{\bar{\mathcal{D}}_3}+1)(2S_{\bar{\mathcal{D}}_4}+1)(2S_{\mathcal{D}_1\bar{\mathcal{D}}_3}+1)(2S_{\mathcal{D}_2\bar{\mathcal{D}}_4}+1)$$
$$\times\begin{Bmatrix}0&1&1\\0&m_i&-m_f\end{Bmatrix}\begin{Bmatrix}S_{\mathcal{D}_1}&1&S_{\mathcal{D}_2}\\\frac{1}{2}&\frac{1}{2}&\frac{1}{2}\end{Bmatrix}\begin{Bmatrix}S_{\bar{\mathcal{D}}_3}&1&S_{\bar{\mathcal{D}}_4}\\\frac{1}{2}&\frac{1}{2}&\frac{1}{2}\end{Bmatrix}\begin{Bmatrix}1&0&1\\1&S_{\mathcal{D}_1\bar{\mathcal{D}}_3}&1\end{Bmatrix}$$
$$\times\begin{Bmatrix}1&0&1\\1&S_{\mathcal{D}_2\bar{\mathcal{D}}_4}&1\end{Bmatrix}\begin{Bmatrix}0&1&1\\1&S_{\mathcal{D}_1\bar{\mathcal{D}}_3}&S_{\mathcal{D}_2\bar{\mathcal{D}}_4}\end{Bmatrix}\begin{Bmatrix}S_{\mathcal{D}_2\bar{\mathcal{D}}_4}&S_{\mathcal{D}_1\bar{\mathcal{D}}_3}&0\\S_{\mathcal{D}_2}&S_{\mathcal{D}_1}&1\\S_{\bar{\mathcal{D}}_4}&S_{\bar{\mathcal{D}}_3}&1\end{Bmatrix}$$
$$\times\begin{Bmatrix}\frac{1}{2}&\frac{1}{2}&S_{\mathcal{D}_1}\\\frac{1}{2}&\frac{1}{2}&S_{\bar{\mathcal{D}}_3}\\1&1&S_{\mathcal{D}_1\bar{\mathcal{D}}_3}\end{Bmatrix}\begin{Bmatrix}\frac{1}{2}&\frac{1}{2}&S_{\mathcal{D}_2}\\\frac{1}{2}&\frac{1}{2}&S_{\bar{\mathcal{D}}_4}\\1&1&S_{\mathcal{D}_2\bar{\mathcal{D}}_4}\end{Bmatrix}\bar{f}^{(f)}_{n_i0n_f0}(\omega_1)\mathbf{k}_1\cdot\mathbf{k}_2+(\mathbf{k}_1\leftrightarrow\mathbf{k}_2)\ , \tag{40}$$

where

$$\bar{f}^{(f)}_{n_i0n_f0}(\omega_1)\equiv\int_0^\infty dk\,k^2\frac{\int_0^\infty dp\,p^2\tilde{R}_{\mathcal{D}_1}(p)\tilde{R}_{\mathcal{D}_2}(p)\tilde{R}_\pi(p)\int_0^\infty dp\,p^2\tilde{R}_{\bar{\mathcal{D}}_3}(p)\tilde{R}_{\bar{\mathcal{D}}_4}(p)\tilde{R}_\pi(p)I_i(k)I_f(k)}{[M_i-E_{\mathcal{D}_1\bar{\mathcal{D}}_3}(k)][M_f-E_{\mathcal{D}_2\bar{\mathcal{D}}_4}(k)][M_i-\omega_1-E_{\mathcal{D}_2\bar{\mathcal{D}}_3}(k)]}\ . \tag{41}$$

A small contribution from the rank-2 irreducible tensor $A^2_{-\bar{m}}(\mathbf{k}_1,\mathbf{k}_2)$ is also neglected in (40).

The total QPC amplitude is then

$$\mathcal{M}_{\rm QPC}=\mathcal{M}^{(e)1}_{\rm QPC}+\mathcal{M}^{(e)2}_{\rm QPC}+\mathcal{M}^{(f)}_{\rm QPC} \tag{42}$$

and the total amplitude is

$$\mathcal{M}=\mathcal{M}_{\rm ME}+\mathcal{M}_{\rm QPC}\ . \tag{43}$$

When calculating the transition rates, the amplitude containing the rank-2 irreducible tensor $A^2_{-\bar{m}}(\mathbf{k}_1,\mathbf{k}_2)$ (the part of $\mathcal{M}^{(a)}_{\rm ME}$ containing c_2) does not interfere with the other amplitudes; however, there is interference between the other amplitudes. Thus the phase of the constant c_2 is irrelevant while the magnitude and the phase of the constant c_1 will both affect the final results. Let

$$c_1=|c_1|e^{i\theta}\ . \tag{44}$$

$|c_1|$ and θ are two unknown parameters in the present theory [$|c_2|$ is related to $|c_1|$ by (28)]. We shall take the well-measured rate $\Gamma(\psi'\to J/\psi\pi\pi)$ [6] and distribution $d\Gamma(\psi'\to J/\psi\pi\pi)/dM_{\pi\pi}$ [7] as inputs to determine the two parameters. Figure 2 shows that θ can be determined within the range $-1<\cos\theta<-0.676$ by the datum of $d\Gamma(\psi'\to J/\psi\pi\pi)/dM_{\pi\pi}$. The corresponding values of $|c_1|$ are listed in Table I. With the determined θ and $|c_1|$ we can predict all the $\pi\pi$ transition rates and $M_{\pi\pi}$ distributions in the $b\bar{b}$ system.

The comparison of the calculated rates for $\Upsilon'\to\Upsilon\pi\pi$, $\Upsilon''\to\Upsilon\pi^+\pi^-$, and $\Upsilon''\to\Upsilon'\pi^+\pi^-$ with the experimental data are listed in Table II. We see that the theory is in good agreement with the experiment. The rates obtained from the naive single-channel theory [3] are smaller than the present values and the new experiment data. So that the inclusion of coupled-channel effects does improve the theory.

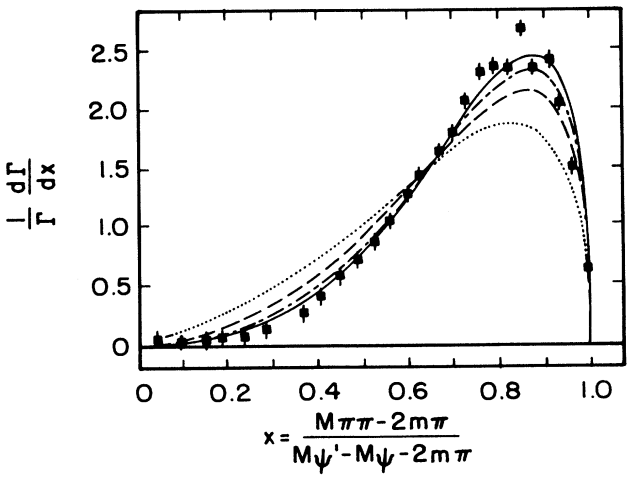

FIG. 2. Comparison of the theoretical curves of $d\Gamma(\psi'\to J\psi\pi\pi)/dM_{\pi\pi}$ with the experiment [7]. The solid, dash-dotted and dotted lines stand for $\cos\theta=-1$, $\cos\theta=-0.676$, and $\cos\theta=1$, respectively. The dashed line is the naive single-channel result for comparison.

TABLE I. Values of $|c_1|$ corresponding to $\cos\theta=-1$ and $\cos\theta=-0.676$.

	$\lvert c_1\rvert^2$
$\cos\theta=-1$	87.8×10^{-6}
$\cos\theta=-0.676$	78.6×10^{-6}

To have an idea of how big the Lipkin-Tuan amplitude ($\mathcal{M}^{(e)1}_{\rm QPC}$) and Moxhay's constant amplitude ($\mathcal{M}^{(e)2}_{\rm QPC}$) are, we list in Table III the rates calculated from the single amplitudes $\mathcal{M}_{\rm ME}$ (with $|c_1|=78.6\times10^{-6}$), $\mathcal{M}^{(e)1}_{\rm QPC}$ and $\mathcal{M}^{(e)2}_{\rm QPC}$, respectively. We see that, for $\Upsilon''\to\Upsilon\pi^+\pi^-$, $\Gamma^{(e)1}_{\rm QPC}$ and $\Gamma^{(e)2}_{\rm QPC}$ are smaller than $\Gamma_{\rm ME}$ by 2 orders of magnitude. The smallness of $\Gamma^{(e)1}_{\rm QPC}$ and $\Gamma^{(e)2}_{\rm QPC}$ is caused by the nodes of the Υ'' wave function, which makes the overlapping integral (22) small. Therefore neither can $\mathcal{M}^{(e)1}_{\rm QPC}$ be dominant nor can $\mathcal{M}^{(e)2}_{\rm QPC}$ be comparable to $\mathcal{M}_{\rm ME}$, so that the Lipkin-Tuan and Moxhay mechanisms for explaining the CLEO data are not realized in the present model.

The predicted $d\Gamma(\Upsilon'\to\Upsilon\pi\pi)/dM_{\pi\pi}$ is shown in Fig. 3, together with the ARGUS datum [8]. We see that the agreement is perfect. In the naive single-channel theory, the approach of Ref. [3] gives the same curve for $d\Gamma(\psi'\to J/\psi\pi\pi)/dM_{\pi\pi}$ and $d\Gamma(\Upsilon'\to\Upsilon\pi\pi)/dM_{\pi\pi}$, which cannot account for the tiny difference between the two data [8]. In Ref. [8] an alternative approach to the hadronization matrix element by Novikov and Shifman [5] is preferred since it contains an unknown parameter κ, and the tiny difference between the two data can be explained by assuming a certain running of κ [8]. Now in our coupled-channel theory we take the same approach to the hadronization matrix element as that in Ref. [3], but coupled-channel corrections to $\psi'\to J/\psi\pi\pi$ and $\Upsilon'\to\Upsilon\pi\pi$ are different due to the different spectra and wave functions. After determining the parameters θ and $|c_1|$ by the inputs $\Gamma(\psi'\to J/\psi\pi\pi)$ [6] and $d\Gamma(\psi'\to J/\psi\pi\pi)/dM_{\pi\pi}$ [7], the curve of $d\Gamma(\Upsilon'\to\Upsilon\pi\pi)/dM_{\pi\pi}$ is definitely predicted. Therefore the present theory predicts exactly the tiny difference between the two data.

The predicted curves of $d\Gamma(\Upsilon''\to\Upsilon\pi^+\pi^-)/dM_{\pi\pi}$ and $d\Gamma(\Upsilon''\to\Upsilon'\pi^+\pi^-)/dM_{\pi\pi}$ are shown in Fig. 4, together with the new CLEO data [9] and the naive single-channel results. We see that $d\Gamma(\Upsilon''\to\Upsilon\pi^+\pi^-)/dM_{\pi\pi}$ does get improved by the coupled-channel corrections. The low-$M_{\pi\pi}$ distribution is increased a little, but it is still too small to account for the CLEO data. The present correction to the low-$M_{\pi\pi}$ distribution comes partly from the *S-D* mixing effects in $\mathcal{M}^{(a)}_{\rm ME}$ and partly from the small $\mathcal{M}_{\rm QPC}$. Our results shows that in the present model the CLEO data cannot be explained simply by coupled-channel effects. Further theoretical investigations are still needed to account for the CLEO data.

TABLE III. Comparison of the rates calculated from different amplitudes. $\Gamma_{\rm ME}$, $\Gamma^{(e)1}_{\rm QPC}$, and $\Gamma^{(e)2}_{\rm QPC}$ are calculated from $\mathcal{M}_{\rm ME}$, $\mathcal{M}^{(e)1}_{\rm QPC}$, and $\mathcal{M}^{(e)2}_{\rm QPC}$, respectively. $|c_1|^2=78.6\times10^{-6}$ is taken for calculating $\Gamma_{\rm ME}$.

	$\Gamma_{\rm ME}$ (keV)	$\Gamma^{(e)1}_{\rm QPC}$ (keV)	$\Gamma^{(e)2}_{\rm QPC}$ (keV)
$\psi'\to J/\psi\pi\pi$	147	0.19	5.1
$\Upsilon'\to\Upsilon\pi\pi$	18	2.4×10^{-3}	0.14
$\Upsilon''\to\Upsilon\pi^+\pi^-$	0.9	9×10^{-13}	1.2×10^{-2}
$\Upsilon''\to\Upsilon'\pi^+\pi^-$	0.5	7×10^{-5}	0.11

IV. DISCUSSIONS AND CONCLUSIONS

We have made a systematic study of the coupled-channel effects in hadronic transitions in the heavy-$Q\bar{Q}$ systems. Several discussions of our results are in order.

(1) In the coupled-channel theory the total $\pi\pi$ transition amplitude is contributed by many Feynman diagrams depicted in Fig. 1. Different diagrams give different behaviors of $M_{\pi\pi}$ distribution, so that the total $M_{\pi\pi}$ distribution is sensitive to the relative strengths of the diagrams. At present there is hardly a reliable model-independent way of determining the relative strengths of the diagrams. Therefore, to examine whether the CLEO data on $\Upsilon''\to\Upsilon\pi^+\pi^-$ can be explained simply by coupled-channel effects in the conventional sense, quantitative calculations based on certian known realistic coupled-channel models are really needed. There are two well-accepted realistic coupled-channel models in the literature, namely, the UQM [2] and the Cornell coupled-channel model [1] (CCCM). Our calculation is based on one of them [2]. It is interesting to discuss whether our conclusion on $\Upsilon''\to\Upsilon\pi^+\pi^-$ is strongly model dependent. The CCCM is different from the UQM both on the mechanism and the results. Compared with the UQM, the CCCM gives larger *S-S* mixings but smaller *S-D* mixings and smaller values of N^2_λ (more continuous sector in the physical state) [1,2]. However, in our calculation we take the data of $\psi'\to J/\psi\pi\pi$ as inputs. Therefore what is relevant is to compare the two models on the ratios $(N^2_{30})_{b\bar{b}}/(N^2_{20})_{c\bar{c}}$ and $(a_{3012}/a_{3030})_{b\bar{b}}/$

TABLE II. Comparison of the calculated rates of $\Upsilon'\to\Upsilon\pi\pi$, $\Upsilon''\to\Upsilon\pi^+\pi^-$, and $\Upsilon''\to\Upsilon'\pi^+\pi^-$ with the experiments. The experimental values are obtained from the data of total widths and branching ratios in Ref. [6].

	Theoretical rates (keV)		Experimental rates (keV)
	$\cos\theta=-1$	$\cos\theta=-0.676$	
$\Upsilon'\to\Upsilon\pi\pi$	14	13	12.0±3.3
$\Upsilon''\to\Upsilon\pi^+\pi^-$	1.1	1.0	0.9±0.3
$\Upsilon''\to\Upsilon'\pi^+\pi^-$	0.1	0.3	0.6±0.3

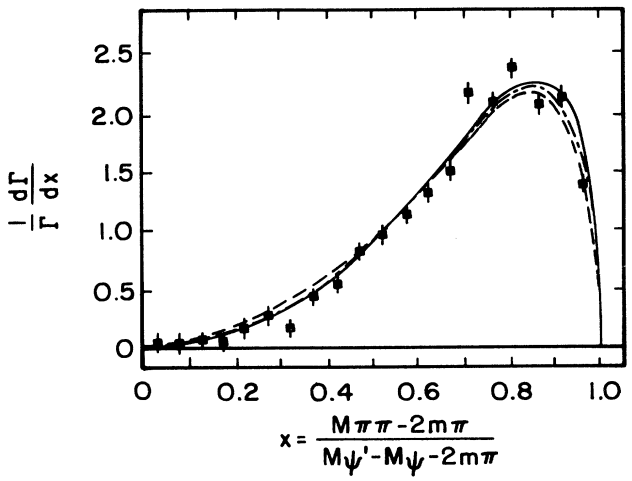

FIG. 3. Comparison of the predicted curve of $d\Gamma(\Upsilon' \to \Upsilon\pi\pi)/dM_{\pi\pi}$ with the ARGUS data [8]. The solid and dash-dotted lines stand for $\cos\theta = -1$ and $\cos\theta = -0.676$, respectively. The dashed line is the naive single-channel result for comparison.

$(a_{2012}/a_{2020})_{c\bar{c}}$. They are listed in Table IV. We see that the difference between the two models is not substantial except that the CCCM gives smaller S-D mixings so that it gives an even smaller low $M_{\pi\pi}$ distribution. Therefore both models seem to lead to the same conclusion that it is unlikely the CLEO data can be explained simply by coupled-channel effects. This is not surprising. We know that the experimental data imply that $\mathcal{M}_{\rm QPC}/\mathcal{M}_{\rm ME}$ should be small in the $2S \to 1S\,\pi\pi$ transition in both the $c\bar{c}$ and $b\bar{b}$ systems. Furthermore, the smallness of the experimental value of $\Gamma(\Upsilon'' \to \Upsilon\pi^+\pi^-)$ (despite the big phase space) implies that $\mathcal{M}_{\rm ME}$ in the $3S \to 1S\,\pi\pi$ transition should be, by some means, suppressed relative to that in the $2S \to 1S\,\pi\pi$ transition. In the present nonrelativistic potential model description of the heavy-quarkonium systems, $\mathcal{M}_{\rm ME}$ is described by a certain overlapping integral related to the initial-state quarkonium wave function. Theoretically, $\mathcal{M}_{\rm ME}$ in $3S \to 1S\,\pi\pi$ is really very much suppressed by the nodes of the $3S$-state wave function [3]. It is this fact that stimulates people to think that coupled-channel effects may explain the CLEO data if $\mathcal{M}_{\rm QPC}$ is not suppressed [13,14]. However, at present, the known successful coupled-channel models (e.g., UQM and CCCM) are all constructed based on the nonrelativistic potential model description of the heavy-quarkonium systems and the coupling between the heavy-quarkonium and its decay channel is described by a certain overlapping integral related to the quarkonium wave function [e.g., Eq. (22) in the UQM]. This is a common feature of this kind of coupled-channel models, although the specific forms of the overlapping integrals are different from model to model. Now the nodes of the $3S$-state wave function not only suppresses $\mathcal{M}_{\rm ME}$ but suppresses $\mathcal{M}_{\rm QPC}$ as well. This is the reason why the CLEO data can hardly be explained simply by coupled-channel effects described by such kind of realistic coupled-channel models such as UQM and CCCM.

(2) The general structure of the $\pi\pi$ transition amplitudes has been studied by Brown and Cahn [26] based on PCAC and the soft-pion technique. An important conclusion is that when we take $\mathbf{k}_1, \mathbf{k}_2 \to 0$, the only nonvanishing term in the amplitude is the σ term, which is proportional to m_π^2 and is thus small. In our result the constant amplitude $\mathcal{M}_{\rm QPC}^{(e)2}$ is really very small compared with $\mathcal{M}_{\rm ME}$ (cf. Table III), so that our result is consistent with the general structure in Ref. [26]. An assumption of a large constant amplitude will not be consistent with Ref. [26].

(3) Comparing the predicted results of $\Gamma(\Upsilon' \to \Upsilon\pi\pi)$ in Ref. [21] and in Table II of this paper, we see that the inclusion of $\mathcal{M}_{\rm ME}^{(b)} + \mathcal{M}_{\rm QPC}$ serves to reduce the rate. In Ref. [4] the rate of $\psi(3770) \to J/\psi\,\pi\pi$ is studied by taking into account of only $\mathcal{M}_{\rm ME}^{(a)}$. The result is larger than the experimental value by a factor of 2–3. This deviation may be

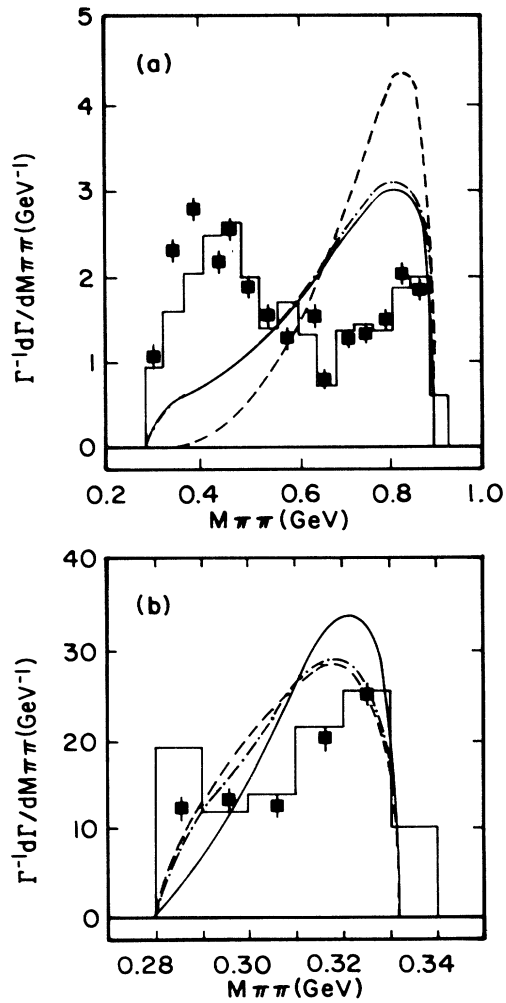

FIG. 4. Comparison of the predicted curves of $d\Gamma(\Upsilon'' \to \Upsilon\pi^+\pi^-)/dM_{\pi\pi}$ and $d\Gamma(\Upsilon'' \to \Upsilon'\pi^+\pi^-)/dM_{\pi\pi}$ with the CLEO data [9]. The solid and dashed-dotted lines stand for $\cos\theta = -1$ and $\cos\theta = -0.676$, respectively. The dashed line is the naive single-channel result for comparison. (a) $\Upsilon'' \to \Upsilon\pi^+\pi^-$, (b) $\Upsilon'' \to \Upsilon'\pi^+\pi^-$.

TABLE IV. Comparison of the Cornell coupled-channel model (CCCM) with the UQM on the ratios $(N^2_{30})_{b\bar{b}}/(N^2_{20})_{c\bar{c}}$ and $(a_{3012}/a_{3030})_{b\bar{b}}/(a_{2012}/a_{2020})_{c\bar{c}}$ obtained from Refs. [1] and [2].

	$\frac{(N^2_{30})_{b\bar{b}}}{(N^2_{20})_{c\bar{c}}}$	$\frac{(a_{3012}/a_{3030})_{b\bar{b}}}{(a_{2012}/a_{2020})_{c\bar{c}}}$
CCCM	1.03	0.07
UQM	1.07	0.16

partly due to the relation (28) which comes from the free-gluon approximation and partly due to the neglect of $\mathcal{M}^{(b)}_{\rm ME}+\mathcal{M}_{\rm QPC}$. Since $\psi(3770)$ lies above the charmed threshold, the effect of $\mathcal{M}^{(b)}_{\rm ME}+\mathcal{M}_{\rm QPC}$ may be more significant. Therefore it is interesting to make a quantitative study of the $\mathcal{M}^{(b)}_{\rm ME}+\mathcal{M}_{\rm QPC}$ correction to $\psi(3770)\to J/\psi\pi\pi$ so that we can see how good the relation (28) really is. This will be given in a separate paper. Of course we expect a more accurate measurement of $\Gamma(\psi(3770)\to J/\psi\pi\pi)$.

(4) Although the four-quark state Υ_1 has not been found in $\Upsilon(4S)$ decays, we cannot rule out the existence of Υ_1 since the estimated branching ratio 1% is rather uncertain. It is based on the oversimplified assumptions that Υ_1 couples with Υ, Υ'', and $\Upsilon(4S)$ with the same strength and $\Upsilon''\to\Upsilon\pi^+\pi^-$ is dominated by the mechanism $\Upsilon''\to\Upsilon_1\pi\to\Upsilon\pi\pi$. Since the wave function of higher radial excitation has more nodes, it is unlikely that the coupling between Υ_1 and $\Upsilon(4S)$ is as strong as that between Υ_1 and Υ or Υ''. Furthermore, from our results in Table II we see that it is also unlikely that $\Upsilon''\to\Upsilon\pi\pi$ is dominated by the Υ_1 mechanism. It is interesting to see whether a combination of the coupled-channel mechanism and the Υ_1 mechanism can explain the CLEO data.

Finally we summarize our main conclusions in this paper.

(1) We have given a general formula (15) for the S-matrix element in heavy-quarkonium decays including multipole-gluon emissions and coupled-channel effects. It can be applied to study various hadronic transition processes and even some other decay processes [19,24].

(2) The inclusion of coupled-channel effects described by the UQM improves the theory of hadronic transitions. By taking the data of $\Gamma(\psi'\to J/\psi\pi\pi)$ and $d\Gamma(\psi'\to J/\psi\pi\pi)/dM_{\pi\pi}$ as inputs to determine the unknown parameters θ and $|c_1|$ in the theory, we have calculated the rates and $M_{\pi\pi}$ distributions of the spin-triplet S-state-to-S-state transitions in the $b\bar{b}$ system and the obtained rates for $\Upsilon'\to\Upsilon\pi\pi$, $\Upsilon''\to\Upsilon\pi^+\pi^-$, and $\Upsilon''\to\Upsilon'\pi^+\pi^-$ (cf. Table II) and the distribution $d\Gamma(\Upsilon'\to\Upsilon\pi\pi)/dM_{\pi\pi}$ (cf. Fig. 3) are all in very good agreement with the experiments. This success of the coupled-channel theory described by the UQM is consistent with those in the study of energy spectra, leptonic widths, etc.

(3) The distribution $d\Gamma(\Upsilon''\to\Upsilon\pi^+\pi^-)/dM_{\pi\pi}$ also gets improved from the coupled-channel corrections but the low-$M_{\pi\pi}$ distribution is still too small to fit the CLEO data (cf. Fig. 4). The smallness of $\mathcal{M}_{\rm QPC}/\mathcal{M}_{\rm ME}$ is due to the nodes of the Υ'' wave function, and from the above discussion we see that UQM and CCCM seem to lead to similar conclusions. Thus we conclude that within the framework of the known realistic coupled-channel models UQM and CCCM, the CLEO data cannot be explained simply by coupled-channel effects. The suggested coupled-channel mechanisms [13,14] for explaining the CLEO data cannot be consistent with all the known successes of the realistic coupled-channel models UQM and CCCM in other heavy-quarkonium processes. Therefore, further theoretical investigation is still needed.

ACKNOWLEDGMENTS

We are grateful to T.-M. Yan and Y. P. Yi for many valuable discussions and would also like to thank N. Byers, C. H. Chang, E. Eichten, H. J. Lipkin, R. D. Peccei, M. E. Peskin, and S. F. Tuan for interesting discussions. One of us (Y.P.K.) would like to thank the Cornell theory group for the kind hospitality extended to him during his visit. This work was partly supported by the U.S. National Science Foundation and the National Natural Science Foundation of China.

*Mailing address.

[1] E. Eichten, K. Gottfried, T. Kinoshita, K. D. Lane, and T.-M. Yan, Phys. Rev. D **17**, 3090 (1978); **21**, 313(E) (1980); **21**, 203 (1980); V. E. Zambetakis, Ph.D. thesis, University of California Report No. UCLA/86/TEP/2; N. Byers (private communication); E. Eichten (private communication).

[2] K. Heikkilä, S. Ono, and N. A. Törnqvist, Phy. Rev. D **29**, 110 (1984); S. Ono and N. A. Törnqvist, Z. Phys. C **23**, 59 (1984); N. A. Törnqvist, Phys. Rev. Lett. **53**, 878 (1984); Acta Phys. Pol. B **16**, 503 (1985).

[3] T.-M. Yan, Phys. Rev. D **22**, 1652 (1980); Y. P. Kuang and T.-M. Yan, *ibid.* **24**, 2874 (1981); Y. P. Kuang, S. F. Tuan, and T.-M. Yan, *ibid.* **37**, 1210 (1988); Y. P. Kuang, in *Heavy Flavor Physics,* Proceedings of the BIMP Symposium, Beijing, China, 1988, edited by C. S. Gao, K. T. Chao, and D. H. Qin (World Scientific, Singapore, 1989); D. S. Liu and Y. P. Kuang, Z. Phys. C **37**, 119 (1987).

[4] Y. P. Kuang and T.-M. Yan, Phys. Rev. D **41**, 155 (1990).

[5] M. B. Voloshin and V. I. Zakharov, Phys. Rev. Lett. **45**, 688 (1980); V. A. Novikov and M. A. Shifman, Z. Phys. C **8**, 43 (1981); M. B. Voloshin, Yad. Fiz. **43**, 1571 (1986) [Sov. J. Nucl. Phys. **43**, 1011 (1986)].

[6] Particle Data Group, G. P. Yost *et al.*, Phys. Lett. B **204**, 1 (1988).

[7] G. S. Abrams *et al.*, Phys. Rev. Lett. **34**, 1181 (1975).

[8] H. Albrecht *et al.*, Z. Phys. C **35**, 283 (1987).

[9] J. Green *et al.*, Phys. Rev. Lett. **49**, 617 (1982); T. Bowcock *et al.*, *ibid.* **58**, 307 (1987); K. Berkelman and D. Cassel (private communications).

[10] M. B. Voloshin, Pis'ma Zh. Eksp. Teor. Fiz. **37**, 58 (1983) [JETP Lett. **37**, 69 (1983)].

[11] T. N. Truong, University of Virginia report (unpublished).

[12] G. Bélanger, T. DeGrand, and P. Moxhay, Phys. Rev. D

39, 257 (1989).
[13] H. J. Lipkin and S. F. Tuan, Phys. Lett. B **206**, 349 (1988).
[14] P. Moxhay, Phys. Rev. D **39**, 3497 (1989).
[15] Y. N. Zhu, Ph. D. thesis, Caltech Report No. CALT-68-1513, 1988.
[16] A. Le Yaouanc, L. Oliver, O. Pene, and J.-C. Raynal, Phys. Rev. D **8**, 2223 (1973).
[17] M. Chaichian and R. Kögerler, Ann. Phys. (N.Y.) **124**, 61 (1980).
[18] D. Gromes, University of Heidelberg Report No. HD-THEP-89-17, 1989 (unpublished).
[19] Y. P. Kuang, Y.P. Yi, and B. Fu, Phys. Rev. D **42**, 2300 (1990).
[20] Even for the $\mathcal{D}$ mesons the leading-order multipole approximation is not so bad since in the potential model the size of $\mathcal{D}$ is not significantly bigger than that of Υ''. The smallness of the higher multipole contribution has been discussed in Ref. [19] and the smallness of the multidipole contributions has been discussed in Ref. [12].
[21] G. Z. Li and Y. P. Kuang, Commun. Theor. Phys. **5**, 79 (1986).
[22] S. Ono, Phys. Rev. D **20**, 2975 (1979); Z. Phys. C **8**, 7 (1981).
[23] D. B. Lichtenberg and J. G. Wills, Nuovo Cimento A **47**, 483 (1978); G. Folgeman, D. B. Lichtenberg, and J. G. Wills, Lett. Nuovo Cimento **26**, 369 (1979).
[24] C. H. Chang, G. P. Chen, Y. P. Kuang, and Y. P. Yi, Phys. Rev. D **42**, 2309 (1990).
[25] S.-H. H. Tye, Phys. Rev. D **13**, 3416 (1976); R. C. Giles and S.-H. H. Tye, Phys. Rev. Lett. **37**, 1175 (1976); Phys. Rev. D **16**, 1079 (1977).
[26] L. S. Brown and R. N. Cahn, Phys. Rev. Lett. **35**, 1 (1975).